An integrated simulation of intermittent heating of multi-zone buildings by heat-pump heating systems with different terminal types

Baoping Xu[1, 2, *], Peihong Jiang[1], Zhuo Chen[1], Qiangang Li[1], Xi Wang[1], Yuying Yan[2, *]

[1] School of Energy, Power and Mechanical Engineering, North China Electric Power University, Beijing 102206, China

[2] Faculty of Engineering, University of Nottingham, Nottingham NG7 2RD, UK

[*]Corresponding authors.

E-mail address: Baoping.Xu@nottingham.ac.uk (B. Xu), yuying.yan@nottingham.ac.uk (Y. Yan)

For submission to:

Applied Thermal Engineering

Abstract

Intermittent heating has been considered to be an effective way to achieve energy savings compared with continuous heating. However, recent studies have found that actual energy savings from intermittent heating vary greatly, depending on actual building conditions, terminals and heating supply systems. For multi-zone buildings adopting heat pumps with specific terminals, a comprehensive analysis of energy savings resulting from intermittent heating still needs to be done. In the present study, an integrated dynamic model is developed by considering the interaction of thermal processes among building envelopes, terminals, and heat pumps. Its reliability is verified in field tests, and a better accuracy was achieved when considering the radiant heat ratio of terminals. On this basis, the model together with a source and terminal control strategy is applied to simulate the thermal behavior of heat pump heating systems for buildings under various conditions. The effect of different terminals and building envelopes on room temperature variation and energy utilization by intermittent heating is analyzed. The simulation results and practical projects indicate that heat pump power consumption under intermittent heating may be lower, close to or even higher than that under continuous heating. The factors that affect the efficient of intermittent heating, including building and system thermal inertia, heat pump operation COP, the radiant heat ratio of terminals, need to be systematically considered. Specifically, fan-coil heating systems could use 16.48% less energy, while radiant floor heating systems consume more energy under

intermittent heating. Heat pumps under continuous heating are more efficient in buildings with radiative heating systems and heavy envelopes.

Keywords: Heat pump; Intermittent heating; Heating terminal; Integrated simulation; Thermal response

1. Introduction

In 2020, the total space that was heated in northern urban China was 15.6 billion m^2, and the energy used for heating was 214 million tce/a (ton of standard coal equivalent per year), accounting for 20% of the total building energy consumption in China [1]. It is expected that the area to be heated in northern urban China will reach 20 billion m^2 in the near future [2]. Since the Chinese government proposes that CO_2 emissions peak around 2030 and that CO_2 emissions are neutralized around 2060 [3], the adoption of effective energy saving measures that aim to control the growth of heating energy consumption is important. For some urban buildings that have difficulty connecting to district heating networks, about 20% of all urban buildings, Jiang et al. [2] proposed that electric heat pumps could be used as heating supply devices, to obtain a higher efficiency than gas boilers. Apart from extremely cold areas where outdoor temperatures can be as low as -20 °C, air source heat pumps (ASHPs) have great application potential for heating buildings across most of China. In addition, intermittent heating has been considered to have a high energy saving rate compared with continuous heating [4], especially for office buildings which have a more defined operating schedule and longer unoccupied periods than residential buildings [5].

Many studies into intermittent heating have been conducted recently, with varying results and views of the energy saving potential. The possibility exists that intermittent heating, when compared to continuous heating, can provide: significant energy savings [6-9]; about the same [4,10,11]; or have higher energy consumption [12]. For example, Deng et al. [9] investigated the use of thermostat setback and occupancy control in office buildings using EnergyPlus simulations and actual tests. According to the results, energy consumption could be reduced by 30% with thermostat setback control. However, an on-site measurement carried out on a residence in Cambridgeshire, England, indicated that the energy saving rate was only about 5% compared with the continuous heating system [4]. In addition, Benakopoulos et al. [10] pointed out that intermittent heating requires a high supply-temperature to ensure a rapid reheating process, and according to the specific building case results, a continuous low-temperature control strategy resulted in similar energy savings to intermittent heating, and secured a low supply and return temperature to the district heating network. In contrast, a comparative study of continuous versus intermittent heating performed in Amman, Jordan [12], found that more comfort and more fuel saving, and lower initial and running costs, were achieved when continuous heating at low temperature was adopted.

Considering the variations in energy savings presented in these previous articles, it suggests that intermittent heating savings depend on the factors that affect the efficacy of intermittent heating. These factors include thermal capacity and heat transfer coefficient of the envelope [4, 5, 12, 13], different types of heating terminals [4, 5, 13], the operating characteristics of the heating supply devices, the supply water temperature [10, 8], and the control strategy [5, 8, 13], etc. The prior studies just focus on some of these impact factors while ignoring the others. As far as the different heating terminals are concerned, various numerical analysis, experimental studies and field tests have been conducted in the past 10 years, to assess the heating characteristics of air conditioner, radiator, and radiant floor [14-16]. Hu et al. [15] conducted an experimental study to evaluate the heating performance of different heating terminals used in heat pump heating system. Wang et al. [14] built a dynamic heat transfer model based on thermal-electrical analogy to compare the convective and radiative heating systems in intermittent heating.

However, there were few discussions on the variation of heating supply device's efficiency under different operating modes. By adopting intermittent heating, the reheating process requires a higher supply temperature to perform quickly when the buildings are reheated to increase the indoor temperature and secure the expected comfort [10]. For multi-zone buildings adopting ASHPs for space heating with specific terminals (radiators, radiant floors, and fan coils), the question that remains is: what heating strategy is more energy effective, continuous operation at a relatively low temperature, or intermittent operation at a higher temperature? Thus, an integrated building and heating system model would be useful to simulate the dynamic thermal response of the system, and to thus provide a comprehensive understanding of this problem.

Numerical methods [14,17] and R-C (thermal resistance - thermal capacity) models [18] have been widely used by previous researchers to study the dynamic process of intermittent heating. Wang et al. [4] built a two-stage lumped parameter model, and concluded that the system with a small thermal constant time was able to elevate indoor temperature quickly, and had great energy saving potential. The heat storage and release processes of internal walls for intermittently heated rooms were studied by employing CFD techniques [17]. Furthermore, different heating terminals exhibit different intermittent heating performances, including heating capacity and thermal response speed, which further influences the indoor thermal environment and energy performance [5,18,19].

The prior modelling or experimental studies can only reveal information for parts of the intermittent heating system, while there is lack of research taking into account combinations of different heating terminals, building thermal processes, and the heating supply system's operation characteristics, all of which are necessary to analyze a system's thermal properties and energy performance in its entirety. In addition, most of the prior studies adopted an intermittent heating strategy based on an on-off schedule and assumed the local thermostat to be an idealized controller [20]. These studies don't simultaneously consider the strategy of supply water temperature control at the heat source, and thermostatic control at the terminals. Therefore, a coordinated control strategy for the source and terminals is worthy of further investigation.

To address the aforementioned problems and challenges, a systematic simulation platform is developed for evaluating the thermal process and energy performance of heat pump heating systems for multizone buildings with different terminals. The main novelties of this study are: (I) a detailed physical model is built to systematically describe the dynamic thermal processes of heat pumps, multi-zone buildings and heating terminals, in which the room temperature and the heat supply quantity are simultaneously resolved by a series of equations; (II) based on the state space method, the radiant heat ratio of terminals is introduced in the thermal balance equation, and the influence of different terminals on room temperature performance is quantitatively analyzed; (III) the integrated model is incorporated into the operating characteristics of heat pumps and the control strategies of the terminals. Validation and case implementation of the model indicate that, the proposed model can be taken as a virtual platform to conduct systematic simulations for heat pump heating systems under various scenarios, and shed light on the choice of heating mode for different building thermal insulation levels and heating terminals.

The rest of this paper is organized as follows. Section 2 introduces the overview of the proposed model integrating the multi-zone building thermal model, the terminal model, and the ASHP model. Section 3 implements the model and a coordinated source-terminal control strategy (including model predictive control for intermittent heating, supply water temperature control and local thermostat control), to simulate the dynamic thermal process of an ASHP heating system for a typical office building in Beijing. The simulation is carried out for various building envelopes and terminals. In Section 4, the validation for the proposed method is presented, and the dynamic thermal characteristics of the ASHP heating system is analyzed with respect to the effect of varying the radiant heat ratio, the room temperature response parameters and the energy saving rate. Finally, conclusions and suggestions for how to choose the best heating operation mode for different situations are presented in Section 5.

2. The modeling approach

The integrated model consists of three parts: a multi-zone building thermal model, a terminal model and a heat pump model. The integrated model systematically describes the dynamic thermal processes of an entire heating system, by considering the influencing mechanisms of different heating terminals on the multi-zone indoor thermal environment, and the operating characteristics of ASHPs.

2.1 Building thermal model

There are some well-known building energy simulation tools with advanced modeling capabilities, such as TRNSYS, EnergyPlus, Modelica, DeST, and etc. However, when it comes to control strategy analysis, an accurate prediction of room temperature variations during response process will be particularly important. One of the challenges is that the room temperature and the heating supply quantity of the terminals exist in both the building thermal model and the terminal model. Some approximations have been adopted for decoupling. Taking multizone building model (Type 56) of Trnsys as an example [21], it is required to define or input heat power of the heating device to calculate the dynamic room temperature. This approach is appropriate for electric heating devices or when the heating supply quantity of the terminal is already known or calculated. However, in district hot water heating systems, the room temperature and the heating supply quantity of the terminals were interacted and influenced by variations of supply water temperature and flowrate, which should be simultaneously resolved.

In this study, the building thermal model was built based on the core algorithm of DeST [22], which successfully passed the ASHRAE-140 standard test. To the best of our knowledge, heat emitting from a terminal device is taken as convective heat in the heat balance equation of indoor air in current platform of DeST. The above-mentioned simulation method is applicable to convective heating terminals. But for convective-radiant heating terminals such as radiators, the method cannot reflect radiation characteristics of the heat transfer between heating terminals and building envelopes, which causes a certain deviation between dynamic simulation results and the actual room temperature variations. Therefore, some changes were made in the process of establishing multizone thermal mode, by integrating the ratio of convection heat to radiation heat of terminals, to improve accuracy of the dynamic simulation.

Accounting for the convection and radiation-heat of terminals is very important for an accurate analysis of the thermal performance of buildings. The differences in the heat transfer process between typical terminals and buildings are shown in Fig.1. Radiators emit heat by convection and radiation, while fan coils affect the temperature of indoor air by convective heat transfer, and radiant floors emit heat mainly by radiation. Therefore, a definition of the radiant ratio (r) of heat emitted from terminals is proposed and introduced in the following thermal-balance equation for indoor air.

$$\begin{aligned} C_{p,a}\rho_a V_a \frac{dT_a(t)}{dt} = & \sum_{i=1}^{n} h_i f_i (T_i(t) - T_a(t)) + C_{p,a}\rho_a G_{out}(t)(T_{out}(t) - T_a(t)) \\ & + \sum_j C_{p,a}\rho_a G_{adj}(t)(T_j(t) - T_a(t)) + Q_{in,1}(t) + (1-r)Q_{term}(t) \end{aligned} \quad (1)$$

where $C_{p,a}\rho_a V_a$ represents the total heat capacity of indoor air, J/K; T_a is the indoor air temperature, ^{o}C; h_i stands for the convective heat transfer coefficient between the interior surface i and the air, W/(m^2·K); f_i denotes the area of the interior surface i, m^2; T_i represents the temperature of surface i, ^{o}C; G_{out} and G_{adj} is the air exchange rate between the room and the outdoors, and the room and adjacent rooms respectively, m^3/s; T_{out} is the outdoor air temperature, ^{o}C; T_j is the air temperature in the adjacent room j; $Q_{in,1}$ denotes the convective portion of the internal disturbance, calculated by the calorific value of each person, lighting equipment and computer equipment, W; Q_{term} denotes the heat power from terminals, W; r is the proportion of radiant heat to total heat emitted from terminals; t is the time.

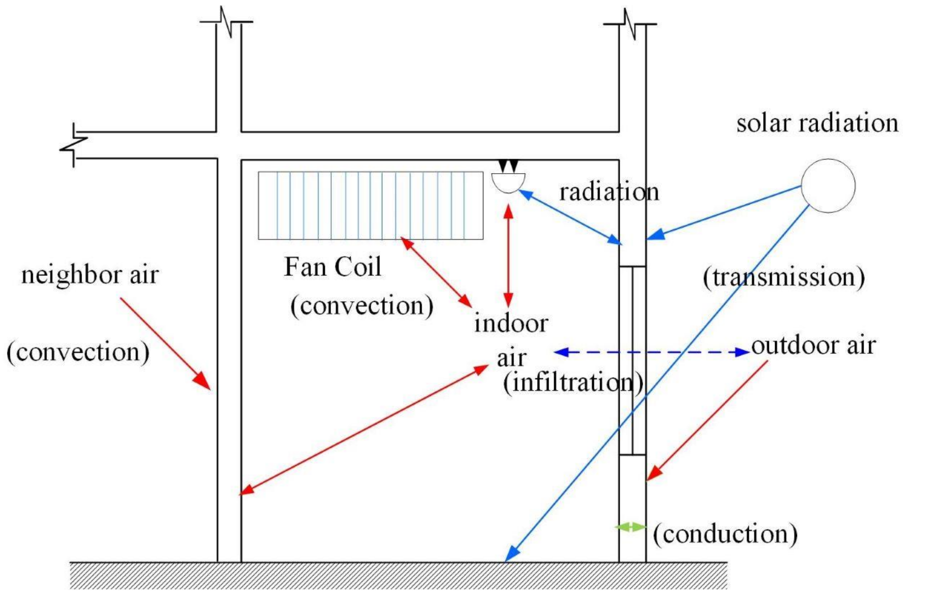

(a) Convective terminal

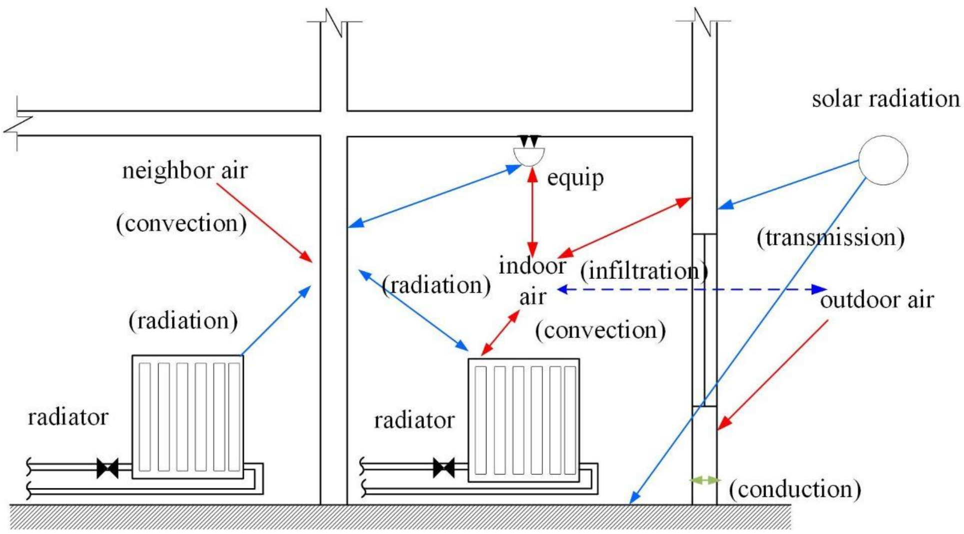

(b) Radiative-convective terminal

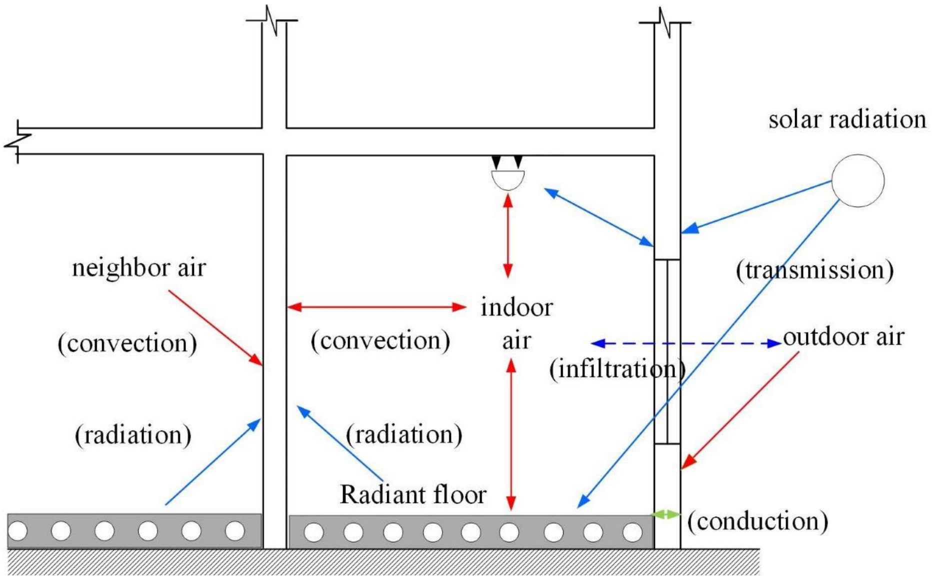

(c) Radiative terminal

Figure 1. Building thermal processes for three typical heating terminals.

Most residential buildings in China are multi-family buildings. The heating demand of residents differs according to the implementation of terminal thermostatic control, and the coupling effect between adjacent residents is greater for radiative heating systems than for convective heating systems. This is because, in radiative heating systems, heat transfer between neighbors is caused by room temperature differences, as well as the indirect effects of radiant heat. It is necessary to consider the radiation effects of terminals between adjacent residences, as described in the following heat balance equation for a partition wall outer surface temperature node T_{n+1}:

$$\frac{1}{2}C_{p,n}\rho_n\Delta x_n\frac{dT_{n+1}}{dt}=h_{n+1}(T_{n+1,a}-T_{n+1})+\frac{\lambda_n}{\Delta x_n}(T_n-T_{n+1})+Q_{rad,n+1}+Q_{in,2}+\alpha\cdot r\cdot Q_{term}(t) \quad (2)$$

where $C_{p,n}$ represents the heat capacity of the discrete layer n, J/(kg·K); ρ_n is the density of the discrete layer n, kg/m^3; Δx stands for the thickness of the discrete layer of the partition wall, m; λ_n stands for the heat conductivity coefficient of the discrete layer n, W/(m·K); $T_{n+1,a}$ denotes the air temperature next to node T_{n+1}, °C; h_{n+1} represents the convective heat transfer coefficient between the outer surface of the partition wall and the air in the neighboring room, W/m^2; $Q_{rad,n+1}$ is the solar gain by node T_{n+1}, calculated by the solar radiation penetrating through the window, W; $Q_{in,2}$ denotes the radiant portion of internal disturbance obtained by node T_{n+1}, calculated by the calorific value of a person, lighting equipment and other exothermic equipment, W; α is the proportion of terminal radiant heat obtained by the partition wall outer surface.

The thermal processes within a building can be described with the state space method [23]:

$$C \cdot \dot{\theta}(t) = A \cdot \theta(t) + B \cdot H(t) \tag{3}$$

where θ is an N-dimensional column vector describing the temperature of all nodes in the state space; $\dot{\theta}$ represents the derivative of θ with respect to time; C is a diagonal matrix describing the thermal capacity of all nodes; A is an $N \times N$ symmetric matrix describing heat conduction, heat convection and long wave heat radiation among all nodes; B is an $N \times M$ matrix describing the impact of the M heat disturbances on the node temperatures; H is an M-dimensional column vector standing for the M heat disturbances, including outdoor temperature, solar radiation, indoor casual gains, heat input from terminals, heat disturbance from adjacent rooms and infiltration or ventilation through openings; C and A depend on the building structures and B depends on the thermal boundary conditions. The detailed foundation of Eq. (3) can be found in Ref. [24].

The solar gains of the building, including the solar radiation reaching the outer surface of the building and penetrating through the window to enter the building, were considered in the thermal-balance equations for the outer or inner layer of envelopes. The detail calculation method can be found in Ref [25]. In addition, the thermal model of the building considering thermal bridges can be obtained, by adopting a thermal bridge additional heat loss model and an order reduce method [26].

The difference approach of setting up the dynamic thermal model for systems with different terminals, results in the difference of thermal disturbance incidence matrix B in Eq. (3). Correspondingly, the influence coefficients of heat on room temperature ($\phi_{1,1}$, $\phi_{1,0}$) in Eq. (4) is different for different terminal forms. Detailed simulation results can be found in Section 4.2.

$$T_a(t)=\sum_i e^{\lambda_i \Delta t} T_{ai}(t-\Delta t)+\sum_k\left(\phi_{k,1} u_k(t-\Delta t)+\phi_{k,0} u_k(t)\right) \tag{4}$$

where $T_{ai}(t-\Delta t)$ represents the room temperature component corresponding to the eigenvalue λ_i of the matrix B at the previous time; $\phi_{k,1}$ is the influence coefficient of heat disturbance k on room temperature at the previous time; $\phi_{k,0}$ is the influence coefficient of heat disturbance k on room temperature at the current time; in particular, $\phi_{1,1}$ is the influence coefficient of heat emitted from terminals on room temperature at the previous time; $\phi_{1,0}$ is the influence coefficient of heat emitted from terminals on room temperature at the current time.

2.2 Terminal model

Three typical heating terminals (radiator, radiant floor, and fan coil), are chosen as the research objects, and corresponding dynamic models are built using the lumped parameter method.

2.2.1 Radiator

As shown in Fig. 2, the dynamic model of a radiator can be thought of as a lumped structure from Eulerian perspective. The energy balance of the model is

$$\frac{d\overline{T}_{\mathrm{rad}}(t)}{dt}=\frac{q_{\mathrm{m}}(t)}{\rho_{\mathrm{w}}V_{\mathrm{rad}}}T_{\mathrm{s}}(t)-\frac{q_{\mathrm{m}}(t)}{\rho_{\mathrm{w}}V_{\mathrm{rad}}}T_{\mathrm{re}}(t)-K_{\mathrm{rad}}(\overline{T}_{\mathrm{rad}}(t)-T_{\mathrm{a}}(t)) \quad (5)$$

where K (s^{-1}) denotes the equivalent heat transfer coefficient

$$K_{\mathrm{rad}}(t)=\frac{\alpha(\overline{T}_{\mathrm{rad}}(t)-T_{\mathrm{a}}(t))^{\beta}\cdot F_{\mathrm{rad}}}{c_{\mathrm{w}}\rho_{\mathrm{w}}V_{\mathrm{rad}}} \quad (6)$$

q_{m} is the quality flow rate, kg/s; $\overline{T}_{\mathrm{rad}}$ denotes the average water temperature in the radiator, °C; T_{re} represents the water temperature at the outlet of the radiator, °C; T_{s} represents the water temperature at the inlet of the radiator, °C; α and β are characteristic coefficients of the radiator, which can be gained from standard experiments; F denotes the surface area, m^2; and V_{rad} is the water capacity of the radiator, m^3; c_{w} stands for specific heat capacity of water, J/kg·K; ρ_{w} is water density, $\mathrm{kg/m}^3$. The subscript 'rad' stands for radiator.

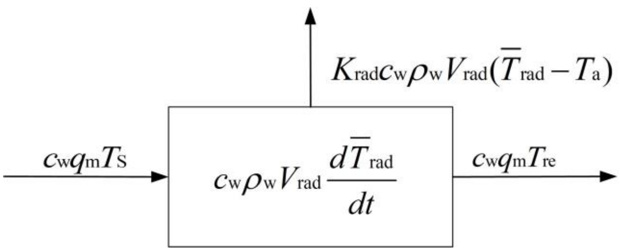

Figure 2. Lumped model of radiator.

The total heat power from the radiator Q_{rad} (W) can be described as

$$Q_{\mathrm{rad}}(t) = K_{\mathrm{rad}} c_{\mathrm{w}} \rho_{\mathrm{w}} V_{\mathrm{rad}} (\bar{T}_{\mathrm{w}}(t) - T_{\mathrm{a}}(t)) \tag{7}$$

2.2.2 Radiant floor

By using the lumped parameter method, the heat conservation equation of a radiant floor can be described as follows:

$$C_{\mathrm{fl}} \frac{d\bar{T}_{\mathrm{flr}}(t)}{dt} = c_{\mathrm{w}} q_m (T_{\mathrm{s}}(t) - T_{\mathrm{re}}(t)) - h_{\mathrm{flr}} F_{\mathrm{flr}} (\bar{T}_{\mathrm{flr}}(t) - T_{\mathrm{a}}(t)) \tag{8}$$

where C_{fl} denotes the total heat capacity of the radiant floor, W/K; $\bar{T}_{\mathrm{flr}}$ is the average temperature of the radiant floor, °C; h_{flr} is the integrated heat transfer coefficient, W/m^2·K; The subscript ‘flr’ stands for radiant floor.

The total heat power from the radiant floor Q_{flr} (W) can be described as

$$Q_{\mathrm{flr}}(t) = h_{\mathrm{flr}} F_{\mathrm{flr}} (\bar{T}_{\mathrm{flr}}(t) - T_{\mathrm{a}}(t)) \tag{9}$$

2.2.3 Fan coil

The model of a fan coil unit adopts the ε-NTU method [27], which has been verified by experiments [28]:

$$Q_{\mathrm{fc}}(t) = \varepsilon(t) C_{\mathrm{fc,min}}(t) (T_{\mathrm{s}}(t) - T_{\mathrm{a}}(t)) \tag{10}$$

$$\varepsilon(t) = 1 - \exp\left(\frac{C_{\mathrm{fc,max}}(t)}{C_{\mathrm{fc,min}}(t)} \cdot NTU^{0.22} \cdot \left(\exp\left(-\frac{C_{\mathrm{fc,min}}(t)}{C_{\mathrm{fc,max}}(t)} NTU^{0.78}\right) - 1\right)\right) \tag{11}$$

where Q_{fc} is the heating capacity of the fan coil, W; ε represents the heat transfer efficiency of the fan coil; $C_{\mathrm{fc,max}}$ and $C_{\mathrm{fc,min}}$ stands for total heat capacity of water and air in the fan coil respectively, W/K; NTU represents the number of heat transfer units of the fan coil.

2.3 Heat pump model

The associated parameters of the heat pump and the building heating system include: the water flow rate, the supply and return water temperature. Ignoring the heat loss of the building's heating supply and return pipe network, the heat pump power consumption W (w) can be calculated as:

$$W(t) = \frac{Q_{\mathrm{tot}}(t)}{COP(t)} = \frac{c_{\mathrm{w}} G_{\mathrm{w,tot}}(t)(T_{\mathrm{s}}(t) - T_{\mathrm{R,tot}}(t))}{COP(t)} \tag{12}$$

where COP is the coefficient of performance (COP) of the ASHP; Q_{tot} is the quantity of heat supplied by the ASHP, W; $G_{\mathrm{w,tot}}$ denotes the total water flow rate, kg/s; $T_{\mathrm{R,tot}}$ stands for the return water temperature at the entrance of the ASHP, °C.

For a certain heat pump, its operating COP depends primarily on the evaporation temperature and condensation temperature. The condensation temperature is related to the supply water temperature, while the evaporation temperature is mainly affected by the outdoor temperature. Therefore, the COP of the ASHP can be expressed as a function of supply temperature and outdoor temperature, as follows:

$$COP(t) = f(T_s(t), T_{out}(t)) \tag{13}$$

The specific functional relationship in Eq. (13) can be built by the parameter identification, based on the product sample data of the ASHP, as shown in Fig. 3.

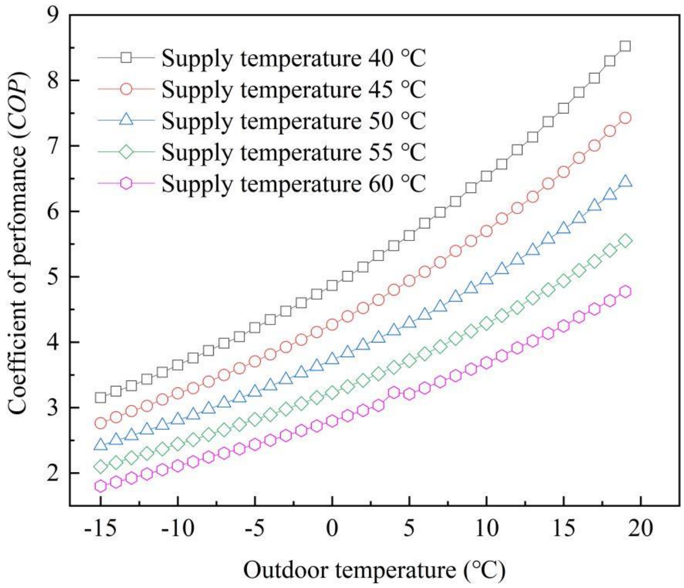

Figure 3. COP of the ASHP under different operating conditions.

2.4 Formulation of an integrated model

The models of the multi-zone building, terminals and the heat pump are not independent. As shown in Fig. 4, the variables in one model always interact with those in the other models. For example, the room temperature and the heating capacity of the terminals exist in both the building thermal model and the terminal model, which can be simultaneously resolved by the group of equations.

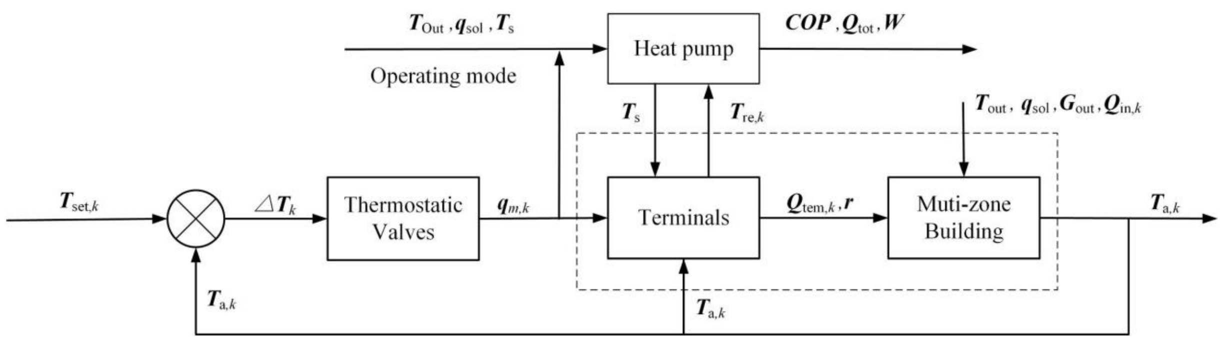

Figure 4. Diagram of the integrated model.

The integrated simulation model developed in this study can be applied for different buildings by inputting different constructer and thermal characteristic parameters of buildings. The integrated model takes weather parameters, supply water temperature, indoor casual heat gains, and the characteristic value of each component as input parameters. For each step in the calculation, the terminal flow rate, outlet water temperature, heating power, and air temperature for each room can be obtained. Then, the time series response of total water flow and return temperature in the building can be calculated according to the mass and heat quantity conservation. Finally, the dynamic electricity consumption of the ASHP can be obtained.

3. Simulated system

3.1 Building description

The simulated building is located in Beijing. The geometry of the building is shown in Fig.5. There are two different room sizes: the size of rooms adjacent to the stairs is 3.25 m × 3 m × 2.8 m, and the size of the other rooms is 4 m × 3 m × 2.8 m. The ratio of window to wall area of the north-south face and east-west face are 0.5 and 0.1, respectively.

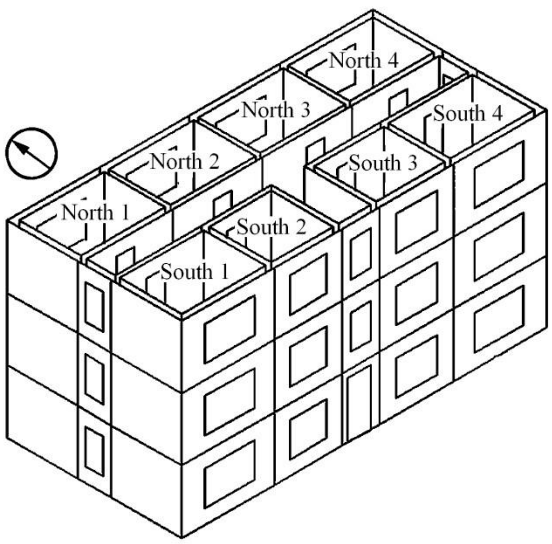

Figure 5. Diagram of the simulated building.

To compare the influence of envelopes with different thermal inertia on the energy saving potential of intermittent heating systems, two kinds of envelopes were simulated: light walls and heavy walls. The heat transfer coefficients of the two kinds of envelopes are given in Table 1, which was confirmed in accordance with Design Standard for Energy Efficiency of Public Buildings [29] and the database in the building performance simulation platform DeST [22]. The g-value of the windows is 0.8. A concept of equivalent slab was applied to solve the problem of dynamic heat transfer through underground zone between building and ground [30]. The temperature outside the equivalent slab is taken as the local average annual surface temperature, which is about 11.8 °C in this study.

Table 1. Physical thermal parameters of building envelopes.

Type of envelope		Thickness /mm	Density /(kg/m^3)	Specific heat /(J/(kg·K))	Heat transfer coefficient /(W/(m^2·K))
Light walls	Exterior walls	340	589	1218	0.37
	Interior walls	170	706	1319	1.19
Heavy walls	Exterior walls	500	1934	841	0.30
	Interior walls	440	2245	895	0.66
Roof		300	1800	879	0.25
Ground		1200	1930	1010	-
Windows		4	2500	837	1.80

For each office room, there is one people during working period (8:00-18:00 from Monday to Friday), and the calorific value of each person is 53 W. The calorific value of lighting equipment and computer equipment are 5 W/m^2 and 10 W/m^2, respectively. The infiltration rate is 0.5 h^{-1}.

For the integrated model, the input weather parameters can be either the measured data or the typical meteorological data, depending on the requirements of the study. In this study, the climate information used in the simulated system is generated from the Typical Meteorological Year Database for Beijing [31], as shown in Fig. 6. The relative humidity was not considered.

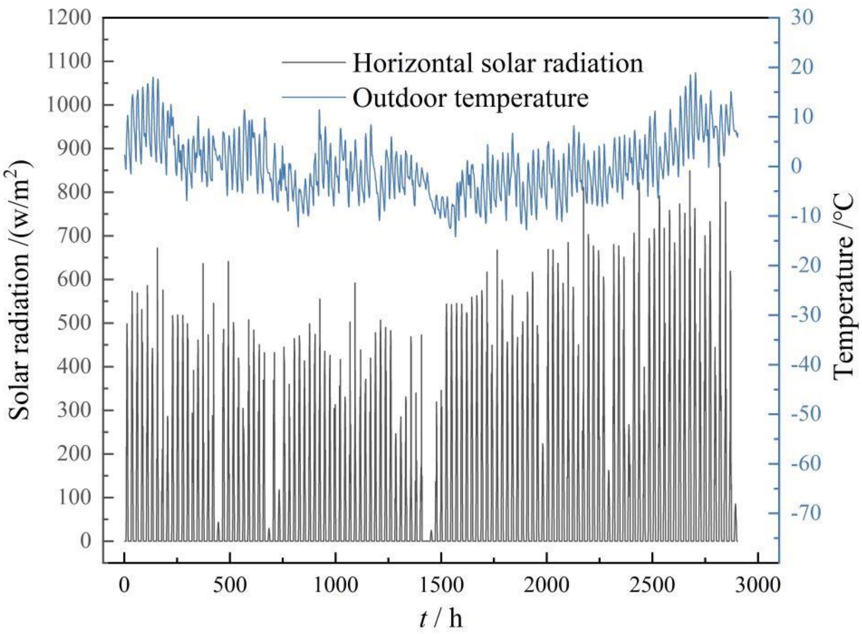

Figure 6. The weather data during a heating season. (Start from 00:00 on Nov 15).

3.2 Terminal heating device parameters

According to the Design Code for Heating Ventilation and Air Conditioning of Civil Buildings (GB 50736-2012) and the Design Standard for Energy Efficiency of Public Buildings (DB 11/687-2015), as well as performance data for the ASHP, different design supply/return water temperatures are considered for different heating terminals under continuous heating and intermittent heating, as shown in Table 2.

Table 2. Design supply and return water temperature for different scenarios.

Type of terminals	Supply/return temp. under intermittent heating (°C)	Supply/return temp. under continuous heating (°C)
Fan-coil	55/40	45/30
Radiator	60/45	50/35
Radiant floor	45/35	40/30

According to the thermal characteristics of different heating terminals, and experimental results [32], the ratios of convection heat and radiation heat over total heat emitted by typical terminals are set as listed in Table 3.

Table 3. The ratios of convection heat and radiation heat over total heat emitted by terminals.

Type of terminals	Ratios of convection heat and radiation heat over total heat emitted by terminals
Fan-coil	1:0
Radiator	0.6:0.4
Radiant floor	0.32:0.68

3.3 Control strategy

3.3.1 Intermittent heating

The goal of using an intermittent heating control strategy is to reduce the runtime of the system while maintaining a comfortable room temperature during working hours. The key factor for an intermittent heating strategy is the optimal start time of the heating system for each working day, which should be predicted.

As shown in Fig. 7, an iterative method is adopted to determine a detailed operating schedule for the heating system for each working day. Firstly, an initial start time is set according to operating experience. Temperature variations for each room during each working day, are obtained from dynamic simulations. Warm-up time is defined as the time needed for the room temperature to reach the lower limit of the comfortable range from when the heating system is started. Thus, the warm-up time can be confirmed by the simulation results of room temperature, and is used as an updated input parameter (heating start-time) to perform the simulation again. By using this iterative method, the optimal start schedule will be obtained.

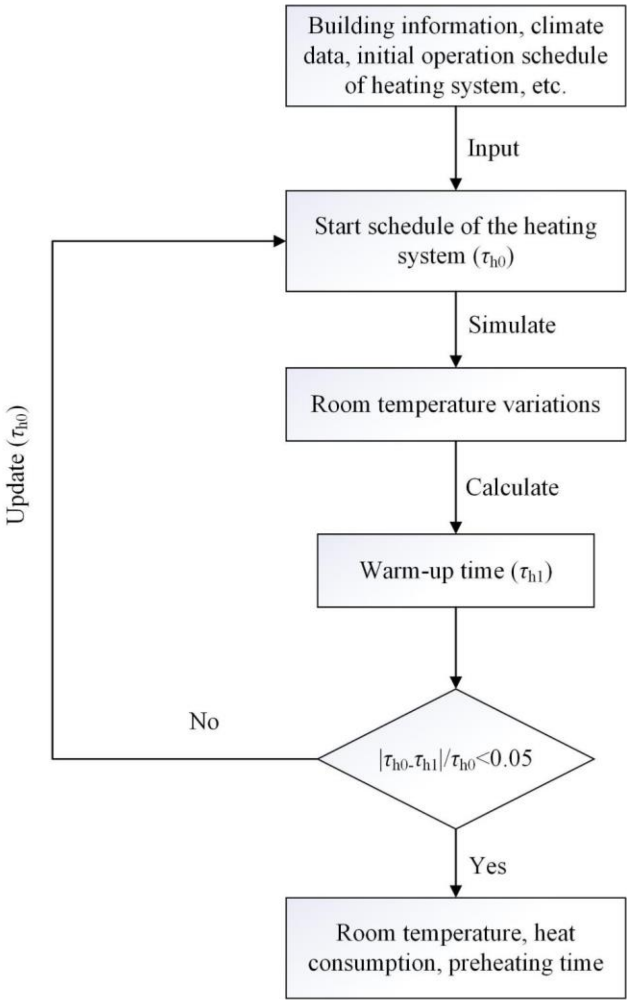

Figure 7. Iterative process for determining the optimal start-time of the intermittent heating system.

3.3.2 Supply water temperature control

The supply water temperature of the building heating system should be adjusted according to the variation of the heating load. The relative heat load (Q_r) can be expressed as a function of outdoor temperature, solar radiation, and ventilation rate.

$$Q_r = \frac{K_{\mathrm{z}} F (T_{\mathrm{a}}' - T_{\mathrm{out}}) + c_{\mathrm{p,a}} \rho_{\mathrm{a}} G_{\mathrm{w,tot}} (T_{\mathrm{a}}' - T_{\mathrm{out}}) - q_{\mathrm{sol}}}{K_{\mathrm{z}} F (T_{\mathrm{a}}' - T_{\mathrm{out}}') + c_{\mathrm{p,a}} \rho_{\mathrm{a}} G_{\mathrm{w,tot}}' (T_{\mathrm{a}}' - T_{\mathrm{out}}') - q_{\mathrm{sol}}'} \tag{14}$$

where K_{z} represents the overall heat transfer coefficient of the building's outer envelope, W/(m^2·K); F denotes surface area of the building's outer envelope, m^2; T_{a}' is the design room temperature, °C; T_{out}' is the design outdoor temperature, °C; q_{sol} stands for solar radiation heat gain, W.

According to the Law of Conservation of Heat, principles of climate compensators for water supply temperature control were built. The heating supply quantity of the heat pump is equal to the total heat emitted by terminals, which will be adjusted based on the variation of the heating load, as described in Eq (15).

$$Q_{\mathrm{r}} = \frac{T_s + T_R - 2T_a}{T_s' + T_R' - 2T_a'} = G_r \frac{T_s - T_R}{T_s' - T_R'} \tag{15}$$

Then, the supply water temperature can be derived from Eq. (15) to Eq. (16).

$$T_{\mathrm{s}} = T_{\mathrm{a}} + \frac{Q_{\mathrm{r}}}{2}(T_{\mathrm{s}}' + T_{\mathrm{R}}' - 2T_{\mathrm{a}}') + \frac{Q_{\mathrm{r}}}{2G_r}(T_{\mathrm{s}}' - T_{\mathrm{R}}') \tag{16}$$

where T_{s}' is the design temperature of supply water, °C; T_{R}' denotes the design temperature of the return water, °C; $G_{\mathrm{r}} = G_{\mathrm{w,tot}}/G'_{\mathrm{w,tot}}$ is the relative flowrate of the system; $G_{\mathrm{w,tot}}$ is the actual flowrate of the system, kg/s; $G'_{\mathrm{w,tot}}$ is the design flowrate of the system at time t, kg/s.

3.3.3 Thermostatic control

To maintain a comfortable room temperature during working hours, there are thermostatic control valves installed in the inlet of the heating terminals, and a simple control strategy is followed: when room temperature goes above 20 ℃, the valves will be closed; and when the temperature falls below 18 ℃, the valves will be fully open.

3.4 Simulation cases

For the purpose of analyzing the thermal response characteristics and the energy saving rate of intermittent heating with different terminals and different building envelopes, simulations were performed for twelve groups of cases summarized in **Table 4**.

Table4. Simulation cases.

Cases	Type of envelopes	Type of terminals	Operation mode
1	Heavy	Fan coils	Intermittent
2	Light	Fan coils	Intermittent
3	Heavy	Radiators	Intermittent
4	Light	Radiators	Intermittent
5	Heavy	Radiant floor	Intermittent
6	Light	Radiant floor	Intermittent
7	Light	Fan coils	Continuous
8	Light	Radiators	Continuous
9	Light	Radiant floor	Continuous
10	Heavy	Radiators	Continuous
11	Heavy	Fan coils	Continuous
12	Heavy	Radiant floor	Continuous

A program based on the integrated model is established using MATLAB for modelling and simulation. The dynamic simulation can be performed with any time step according to the requirements of the study. We use a simulation time step of 30 min in this study. For each step in the calculation, the terminal flow rate, outlet water temperature, heating power, and air temperature for each room in the building of Fig.5

can be obtained.

4. Results and discussion

4.1 Field tests for model validation

4.1.1 Model validation under various conditions

To test the model, two district heating systems, one in Beijing and another in Tianjin, were investigated in our previous studies [5, 23, 33]. The accuracy of the multi-zone building model was verified by experimental data for different rooms and heating systems under three operation modes. In Mode I, the heating system were regulated intermittently according to a work schedule. In Mode II, the thermostatic valves of terminals were kept on an intermediate setting and self-adjusted to control the room temperature. In mode III, the valve at the heat entrance of the apartment was on-off adjusted to verify the coupling between the apartments in the multizone building heating systems. There was good agreement between the measured and simulated values for the room temperature, return water temperature, and flow rate of the terminals [23].

4.1.2 Comparison with typical simulation tool

In this study, the building thermal model was built based on the core algorithm of DeST, and improved by integrating the ratio of radiant heat of terminals. Therefore, the further validation was mainly focused on the influence of considering or not considering the radiant heat ratio of the terminals. The validation was carried out in a multizone building with a radiator heating system in Beijing. The typical simulation tool DeST was taken for comparison. A northern room on second floor of the building, was chosen for detail validation of the simulated room temperature under intermittent heating mode.

Surface temperature self-record meters (30 min time intervals) were installed at the inlet and outlet pipes of the radiator (Fig.8 (a))., and an ultrasonic flowmeter was installed in the return pipe of the radiator (Fig.8 (b)). Self-recording room temperature meters were installed in the studied room and in all of the neighboring rooms (Fig.8 (c)). These temperature recording meters were placed in the same relative position, one for each room. The meter sensors were placed away from the radiators, and at a height of about 1.5 m. An additional outdoor weather logger was mounted in the leeward and shaded side of the building, to eliminate direct solar and wind radiation (Fig.8 (d)). Table 5 shows the measurement instruments and their parameters used in the field test.

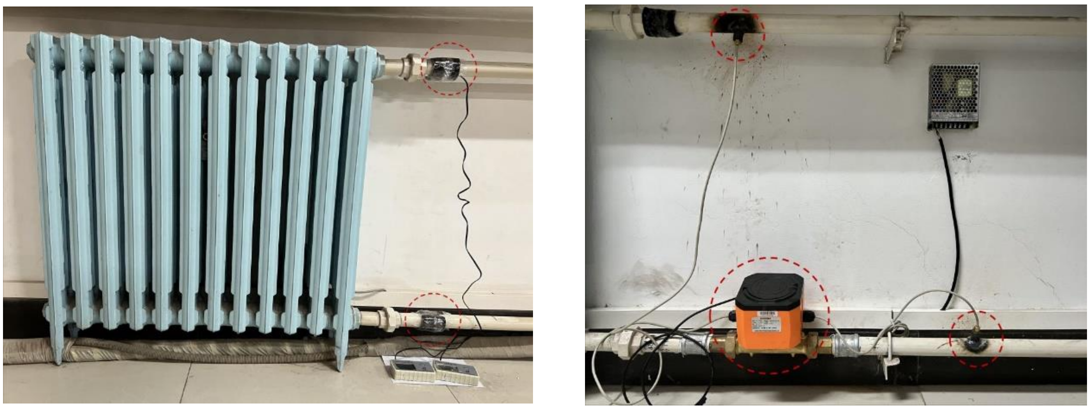

(a) Pipe surface temperature (b) Flowrate and water temperature

(c) Room temperature (d) Outdoor temperature

Figure 8. Field test measurement situation.

Table 5. Parameters of the main measurement instruments.

Instrument	Type	Parameter	Image
Air temperature and humidity self-recording meter	WSZY-1	Ambient temperature in field test (±0.3 ˚C)	

Surface temperature self-recording meter	WZY-1	Surface temperature of the terminal (±0.3 °C)	
Flowmeter	Ultrasonic flowmeter	Flow rate of the terminal (±0.5 %)	
Thermal resistance	Platinum thermistor	Inlet and outlet water temperature (±0.1 °C)	

The experimentally measured neighboring room temperature, outdoor temperature, supply water temperature and radiator flow rate were used as inputs (see Fig. 9) for the model and the simulation tool, and then the simulated room temperatures were compared with the measured values. Solar radiation and indoor casual heat gains can be ignored in the northern empty tested room.

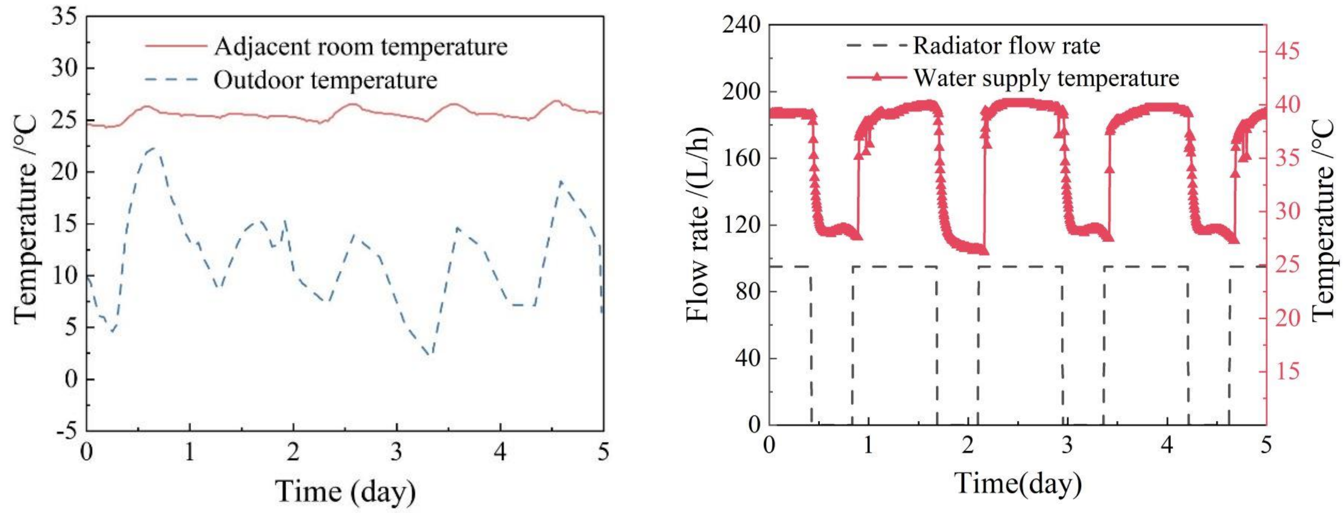

(a) Outdoor temp. and adjacent room temp (b) Supply temperature and flow rate

Figure 9. Input parameters of the validation.

As shown in Fig. 10, the simulation accuracy for room temperature is obviously better when the radiant ratio of the heat emitting from the radiators is considered. The performance of the model is evaluated by four statistical indices, including the coefficient of variation of the root-mean-square error (CV-RMSE), the coefficient of variation of the standard deviation (CV-STD), the normalized mean square error

(NMSE), and the mean-square error (MSE). The first two indices are recommended by the ASHRAE Guideline 14-2014 [34], and the last two indices are also usually used to characterize the calculation accuracy. The evaluation results listed in Table 6 demonstrate the effectiveness of the proposed model in this study.

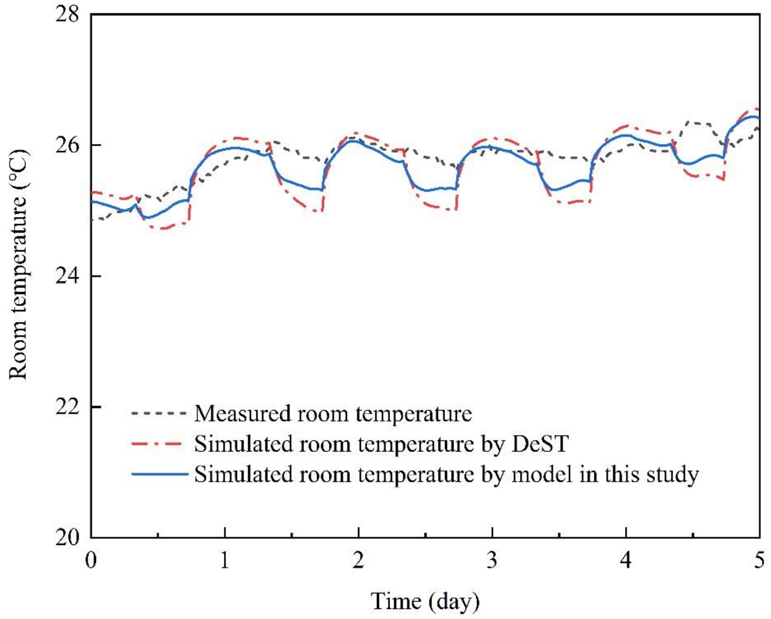

Figure 10. Comparison of the simulated and measured room temperatures.

Table 6. Model performance evaluation results.

	CV-RMSE	CV-STD	NMSE	MSE
Results by model in this study	0.0152	0.0384	0.1009	0.1398
Results by DeST	0.0199	0.0429	0.1733	0.2403

The formula for NMSE calculation is

$$NMSE = \frac{\sum (y_i - \hat{y}_i)^2}{\sum (y_i - \bar{y}_i)^2} \tag{17}$$

The formula for MSE calculation is

$$MSE = \frac{\sum (y_i - \hat{y}_i)^2}{n} \tag{18}$$

where $\hat{y}$ is the simulation predicted data, y is the utility data used for calibration, $\bar{y}$ is the arithmetic mean of the sample of n observations, n is the number of data points.

4.2 The effect of varying the radiant heat ratio

From the simulation results, it can be seen that the influence coefficients $\phi_{1,1}$ and $\phi_{1,0}$ in Eq. (13) both have a linear relationship with the radiant heat ratio of terminals. As shown in Fig. 11, with the increase of radiant heat ratio, the influence coefficient of heat emitted from terminals on the room temperature at the current moment and the previous moment both decreases. Fig. 12 indicates that, the room temperature response rate decreases with the increase of radiant heat ratio, at the initial stage of heating system restart.

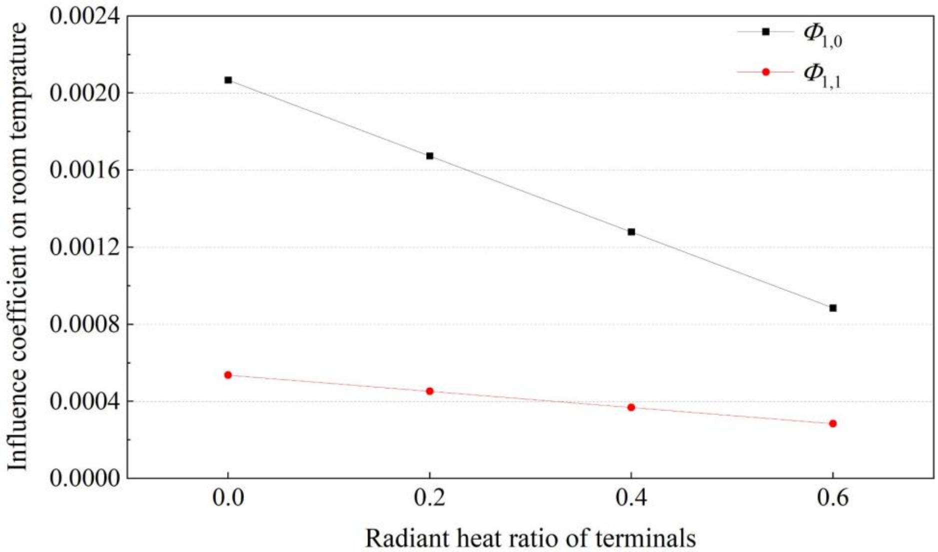

Figure 11. Influence coefficient varies with the radiant heat ratio of terminals.

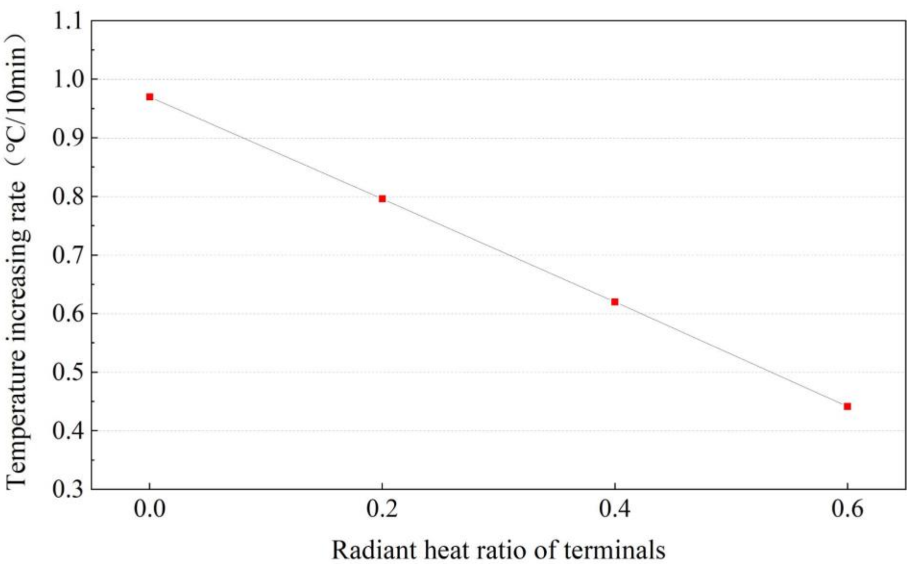

Figure 12. Room temperature rise rate varies with the radiant heat ratio of terminals.

4.3 Room temperature response characteristics

4.3.1 Influence of different heating terminals

A northern room on first floor of the building, was chosen for analysis. **Figure 13** shows the simulated results of room temperature variations during a typical week under daily intermittent heating. Room temperatures fluctuated the most for fan coil heating terminals. After reaching the target room temperature, frequent switching of the regulating valve leads to frequent fluctuations in the room temperature. When a radiant floor is used as the heating terminal, the room temperature fluctuation is the least. That is, the larger the radiant heat ratio of terminals, the slower the thermal response speed of the system, and the smaller the temperature fluctuation during intermittent heating.

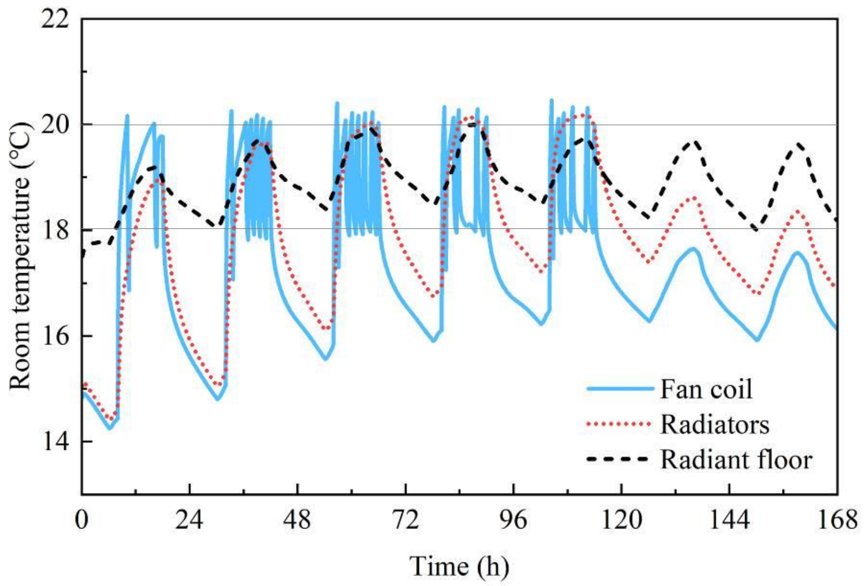

Figure 13. Variation in room temperature for different terminals during a typical week under daily intermittent heating.

Table 7 lists the room temperature response parameters under daily intermittent heating during a typical week (from Jan 1 to Jan 7). The warm-up time for radiator heating systems is obviously longer than that for fan-coil heating systems, and the time needed on Monday morning is much longer than that needed on Tuesday to Friday mornings. Due to the large thermal inertia of radiant floor heating systems, the room temperature variation is minimal, and there is almost no need to preheat during the daily intermittent heating process.

Table 7. Room temperature response parameters for different terminals under daily intermittent heating.

		Fan coils	Radiators	Radiant floor
Monday	Warm-up time /h	0.33	4	0
	Temperature increasing rate /(°C/h)	10.79	0.86	-
Tuesday	Warm-up time /h	0.2	1.83	0
	Temperature increasing rate /(°C/h)	14.72	1.47	-
Wednesday	Warm-up time /h	0.13	0.83	0
	Temperature increasing rate /(°C/h)	16.26	2.22	-
Thursday	Warm-up time /h	0.12	0.47	0
	Temperature increasing rate /(°C/h)	16.56	2.31	-
Friday	Warm-up time /h	0.09	0.23	0
	Temperature increasing rate /(°C/h)	16.62	2.51	-

4.3.2 Influence of different building thermal inertias

Figure 14 shows the simulation results of the room temperature response for buildings with different types of envelopes in the case of long-term intermittent heating where the heating system is re-started at 8 am after a long period of no heating (e.g., the spring festival). Three typical heating terminals (fan coils, radiators, and radiant floor) were both considered and analyzed for the light and heavy envelopes.

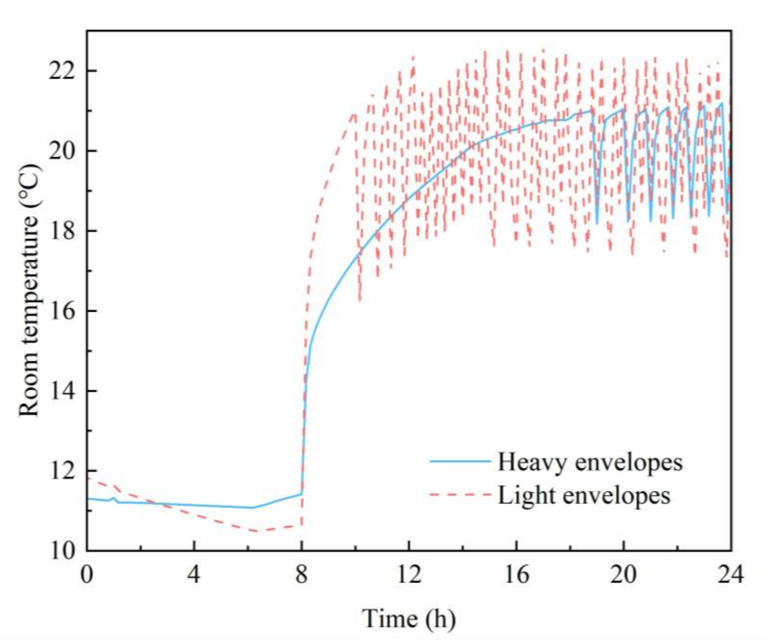

(a) Fan coil

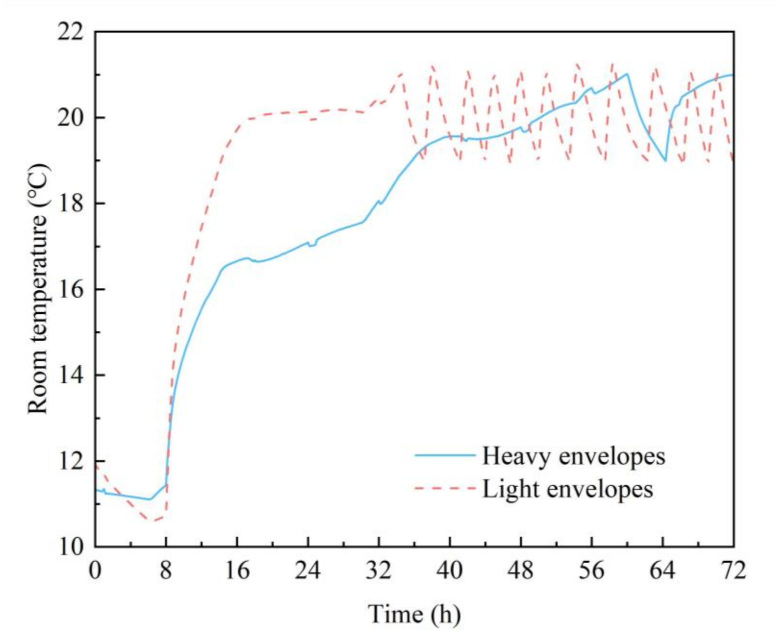

(b) Radiator

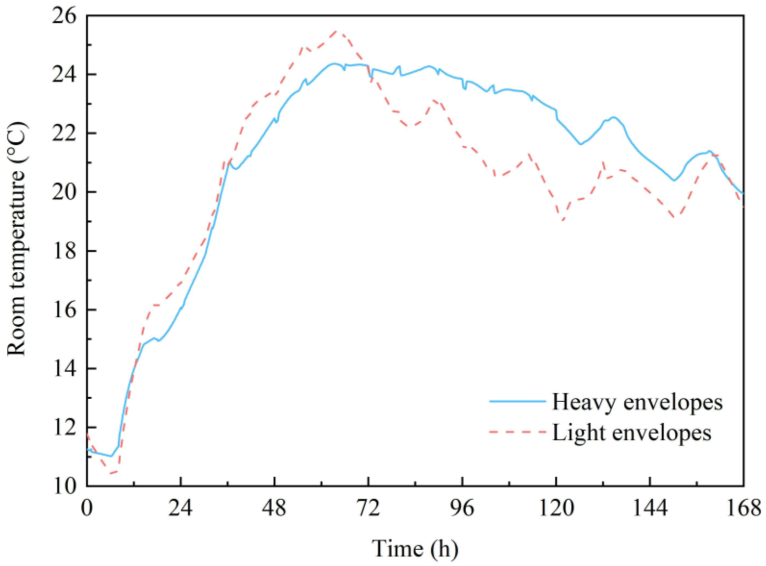

(c) Radiant floor

Figure 14. Variation in room temperature in buildings with different envelopes on typical days under long-term intermittent heating.

The room temperature response parameters for buildings with different kinds of envelopes and terminals are listed in **Table 8.**

Table 8. Thermal response parameters for buildings with different envelopes.

Type of envelopes	Type of terminals	Response time* /h	Temperature increasing rate / (°C/h)	Time constant** / h
Heavy	Fan coils	3.50	1.94	1.83
Light	Fan coils	1.33	5.65	0.67
Heavy	Radiators	25.50	0.26	6.17
Light	Radiators	5.17	1.43	2.83
Heavy	Radiant floor	30.13	0.22	29.50
Light	Radiant floor	28.83	0.26	29.00

*: Response time is the time that it takes from heating system start-up to reach a room temperature at the lower limit of the comfort zone, in the case of long-term intermittent heating.

**: Time constant is the time required for the indoor temperature to rise through approximately 63 percent of its total increasing amplitude since the heating system is started.

From **Table 8**, it can be seen that the response time for buildings with heavy envelopes is longer (3.5 h-30.1 h) than for buildings with light envelopes (1.33 h-28.83 h), and that the temperature increasing rate for buildings with heavy envelopes is slower than that for buildings with light envelopes. In other words, the greater the thermal inertia, the slower the thermal response and the smaller the fluctuation in room temperature. When the heating terminal is a radiant floor, the difference in room temperature response parameters between the two kinds of building envelopes is the least. In contrast, when the heating terminals are radiators, the difference in room temperature response parameters between those two kinds of building envelopes is the highest.

4.4 Factors affecting energy savings with intermittent heating

4.4.1 Influence of different heating terminals

For buildings with light envelopes, the power consumptions of heat pumps for buildings with different kinds of terminals in the first heating month, are compared in **Fig. 15**. The average COP of the system under different scenarios was listed in **Table 9**.

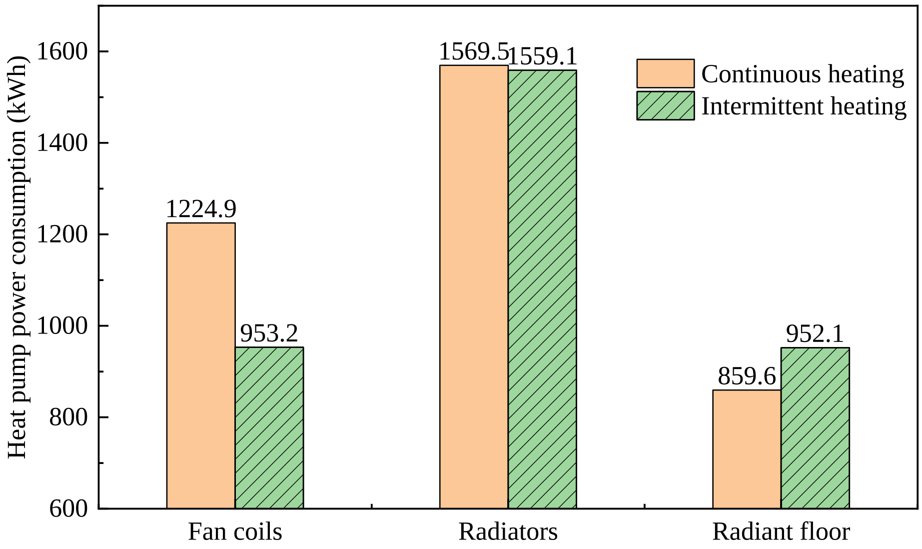

Figure 15. Heat pump power consumption with different heating terminals under intermittent heating versus continuous heating.

Table 9. The average COP of the system under different scenarios.

	Fan Coils	Radiators	Radiant floor
Intermittent heating	2.92	2.52	3.85
Continuous heating	3.85	3.36	4.38

These results contradict the generally accepted notion that intermittent heating will obviously uses less energy. Instead, the results of the calculation show that, compared with the power consumption of the heat pump under continuous heating, the power consumption of the heat pump under intermittent heating may be lower, similar or even higher, depending on the terminal type. Specifically, under intermittent heating, fan-coil heating systems can significantly achieve energy savings (with an energy saving rate of 16.48%), while radiant floor heating systems consume more energy. The heat pump power consumption in radiator heating systems for intermittent heating and continuous heating is very similar. Therefore, from an energy saving perspective, an intermittent heating strategy is more suitable for heating systems with convective terminals.

4.4.2 Influence of different building thermal inertias

For radiator heating systems, the first month power consumption of heat pumps for buildings with different kinds of envelopes are compared in **Fig. 16**.

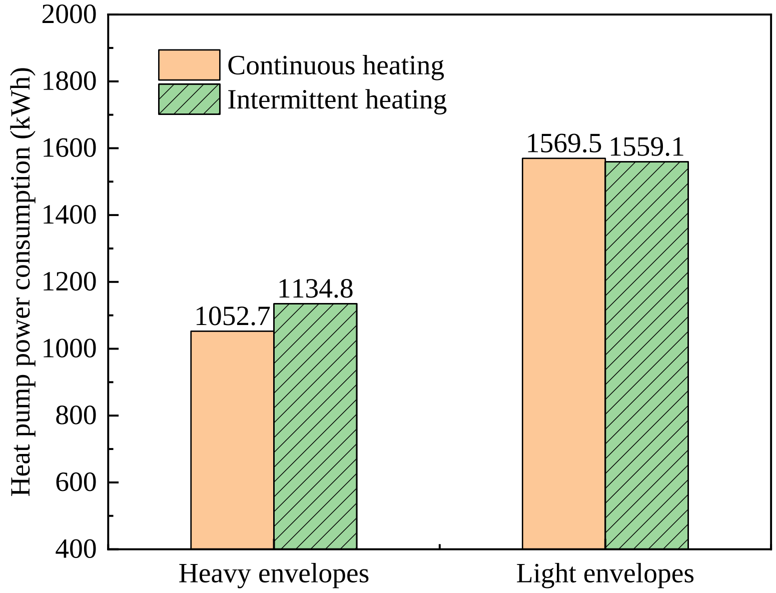

Figure 16. Heat pump power consumption for buildings with different envelopes under intermittent heating or continuous heating.

As shown in Fig. 16, heat pump power consumption is similar under intermittent heating versus continuous heating for buildings with light envelopes, while a heat pump operated continuously is more energy efficient for buildings with heavy envelopes. These results indicate that intermittent operation is more suitable for buildings with less thermal inertia.

4.5 Analysis on practical examples

Two typical practical examples, concerning about the comparative analysis of continuous versus intermittent heating performed in Northern China, are given. The operation data shows a good agreement with the simulation results.

The first project is a ground source heat pump heating system with radiative heating terminals (radiant floors) for a passive energy-saving house in Qingdao [35]. The building thermal parameters are listed in Table 9. When the outdoor climate conditions are basically similar, as shown in Fig. 16, the average daily power consumption for the heat pump is approximately 1238 kWh under 24-hour continuous operation mode with a lower supply water temperature of 35 ^{o}C, and the average daily power consumption is about 1432 kWh under 10-hour intermittent operation mode with a higher supply water temperature of 40 ^{o}C. Fig. 17 gives the measured room temperature variations under these two operating modes, which can both meet indoor thermal comfort. In this practical case, the continuous operation is more efficient for the heat pump heating system.

Table 10. Thermal parameters of the passive house envelopes.

Envelope types	Heat transfer coefficient (W/(m^2·K))	Structure
Exterior walls	0.17	250 mm rock wool panels
Roof	0.12	430 mm extruded polystyrene panels
Exterior windows	0.8	Triple glazed double insulated aluminum clad low-e glass window
Ground	0.085	200 mm phenolic insulated panels
Partition walls	0.18	250 mm rock wool panels

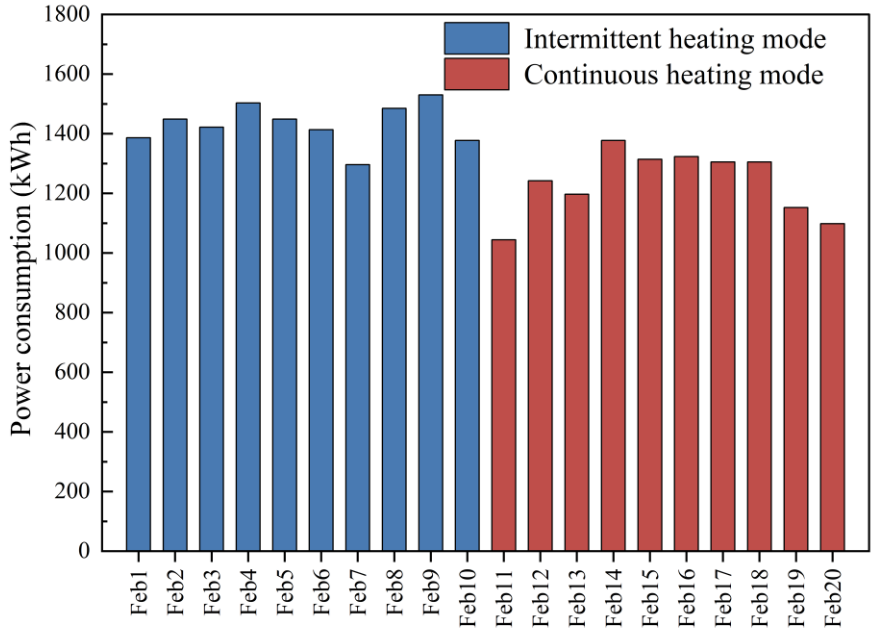

Figure 17. Measured power consumption of heat pump under different heating modes.

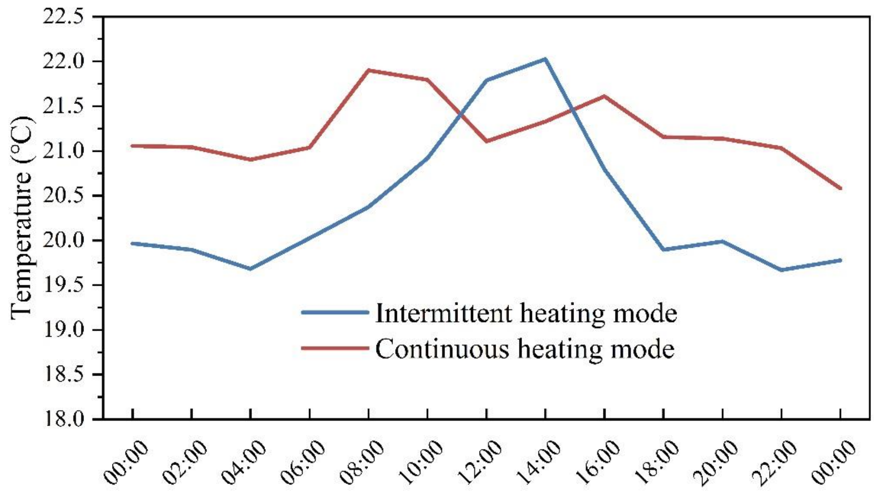

Figure 18. The measured room temperature variations on a typical day under different heating modes.

Field regulation and tests were also carried out in multi-zone buildings of a district radiator heating system in Beijing, China [36]. The envelope structure of the buildings was designed in accordance with Design Standard for Energy Efficiency of

Residential Buildings [37]. As shown in Fig. 19, when the heating system of an apartment was turned off for 8 h, the maximum decrease in room temperature was less than 1 ^{o}C, compared with that of the reference apartment with continuous heating. The results also show that the energy-saving ratio of the intermittent heating system was only about 6% compared with the continuous heating system, which is not significant. Similar results can be found in several other tests of radiator heating systems [4].

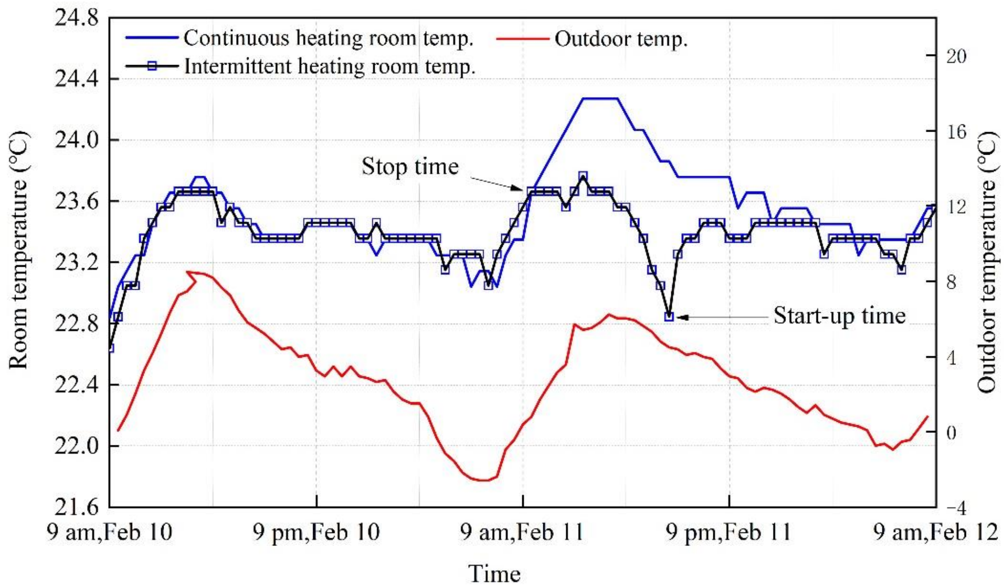

Figure 19. Measured temperature under intermittent versus continuous heating mode.

5. Conclusions

A dynamic integrated model for simulating the thermal process of buildings with heat-pump heating systems was proposed, and its reliability was experimentally verified by field tests. The proposed model was implemented to simulate the thermal performance of heat pump heating systems for office buildings, under intermittent heating and also under continuous heating. The effect of different terminals and building envelopes on room temperature variation and heat pump power consumption was analyzed. The main conclusions are:

(1) The ratio of convection heat to radiation heat of the heating terminal, which was introduced in the dynamic thermal balance equations, is a key parameter to describe the characteristic of heat transfer between the terminal and the building. Field tests demonstrated that the simulated results were closer to the tested values when considering the proposed ratio.

(2) The effect of varying the terminal's radiant heat ratio on room temperature performance was analyzed. When the radiant heat ratio increases from 0 to 0.6, the influence coefficient of heat emitted from terminals on the room temperature at the current moment represents a reduction of 57.1 %.

(3) For buildings with convective terminals (such as fan coils), the warm-up time is 0.17 h to 0.5 h, and for those with convective-radiative terminals (such as radiators), the warm-up time is 0.83 h to 4 h under daily intermittent heating, while there is nearly no need to preheat in buildings with radiative terminals (such as radiant floors).

(4) The response time for buildings with heavy envelopes is 3.5 h to 30.1 h, while it is 1.33 h to 28.8 h for buildings with light envelopes under long-term intermittent heating. When radiative heating terminals are adopted, the influence of different kinds of building envelopes on the temperature response time is the least.

(5) From a comprehensive analysis considering not only the heat consumption but

also the COP variation of the heat pump heating system, the power consumption of heat pumps might be less, close or even more under intermittent heating versus continuous heating. Intermittent heating operation is more appropriate for heating systems with convective terminals and light envelopes, which can achieve an energy saving rate of 16.48% in the simulated case.

Acknowledgments

This research was supported by the National Natural Science Foundation of China (52278106, 51708210), the European research network project (H2020-MSCA-RISE-778104-ThermaSMART), and the China National Key R&D Program (2021YFE0194500). CSC (China Scholarship Council) support for the first author’s research visiting at University of Nottingham, UK.

References

[1] Building Energy Research Center, Tsinghua, Annual research report for the development of building energy saving in China, Beijing: China Building Industry Press, 2022. (in Chinese)

[2] Y. Jiang, S. Hu, Paths to carbon neutrality in China’s building sector, Heat. Ventil. Air Condit. 51 (2021) 1-13. (in Chinese)

[3] Y. Zhang, D. Yan, S. Hu, et al., Modelling of energy consumption and carbon emission from the building construction sector in China, a process-based LCA approach, Energy Pol. 134 (2019) 110949.

[4] Z. Wang, B. Lin, Y. Zhu, Modeling and measurement study on an intermittent heating system of a residence in Cambridgeshire, Build. Environ. 92 (2015) 380-386.

[5] B. Xu, S. Zhou, W. Hu, An intermittent heating strategy by predicting warm-up time for office buildings in Beijing, Energy Build. 55 (2017) 35-42.

[6] G. Fraisse, J. Virgone, C. Menezo, Proposal for a highly intermittent heating law for discontinuously occupied buildings, Proc. Inst. Mech. Eng. 214 (2000) 29-39.

[7] D. Pupeikis, A. Burlingis, V. Stankevicius, Required additional heating power of building during intermittent heating, J. Civ. Eng. Manag. 16 (2010) 141-148.

[8] G. Liu, X. Zhou, J. Yan, et al., A temperature and time-sharing dynamic control approach for space heating of buildings in district heating system, Energy 221 (2021) 119835.

[9] Z. Deng, Q. Chen, Simulating the impact of occupant behavior on energy use of HVAC systems by implementing a behavioral artificial neural network model, Energy Build. 198 (2019) 216-227.

[10] T. Benakopoulos, W. Vergo, M. Tunzi, et al., Energy and cost savings with continuous low temperature heating versus intermittent heating of an office building with district heating, Energy 252 (2022) 124071.

[11] F. Neirotti, M. Noussan, S. Riverso, et al., Analysis of different strategies for lowering the operation temperature in existing district heating networks, Energies 12 (2019) 1-17.

[12] A.A. Badran, A. W. Jaradat, M. N. Bahbouh, Comparative study of continuous versus intermittent heating for local residential building: Case studies in Jordan, Energy Convers. Manag. 65 (2013) 709-714.

[13] C. Hu, R. Xu, X. Meng, A systemic review to improve the intermittent operation efficiency of air-conditioning and heating system, J. Build. Eng. 60 (2022) 105136.

[14] D. Wang, Y. Liu, Y. Wang, J. Liu, Numerical and experimental analysis of floor heat storage and release during an intermittent in-slab floor heating process. Appl. Therm. Eng. 62 (2014) 398-406.

[15] B. Hu, R.Z., Wang, B. Xiao, et al., Performance evaluation of different heating terminals used in air source heat pump system. Int. J. Refrig. 98 (2019), 274-282.

[16] M. Duan, Y., Wu, H. Sun, et al., Intermittent heating performance of different terminals in hot summer and cold winter zone in China based on field test. J. Build. Eng. 43 (2021) 102546.

[17] S. Wang, Y. Kang, Z. Yang, et al., Numerical study on dynamic thermal characteristics and optimum configuration of internal walls for intermittently heated rooms with different heating durations, Appl. Therm. Eng. 155 (2019) 437-448.

[18] Z. Wang, M. Luo, Y. Geng, et al., A model to compare convective and radiant heating systems for intermittent space heating, Appl. Energy 215 (2018) 211-216.

[19] M. Duan, Y. Wu, H. Sun, Z. Yang, W. Shi, B. Lin, Intermittent heating

performance of different terminals in hot summer and cold winter zone in China based on field test, J. Build. Eng. 43 (2021) 102546.

[20] K. Zhang, M. Kummert, Evaluating the impact of thermostat control strategies on the energy flexibility of residential buildings for space heating, Build. Simul. 14 (2021) 1439 -1452.

[21] TRANSSOLAR Energietechnik, Multizone building modeling with type56 and TRNBuild, In Trnsys 18 Documentation, Volume 5, 2017.

[22] D. Yan, X. Zhou, J. An, et al, DeST 3.0: A new-generation building performance simulation platform. Build. Simul. 15 (2022) 1849-1868.

[23] B. Xu, L. Fu, H. Di, Dynamic simulation of space heating systems with radiators controlled by TRVs in buildings, Energy Build. 40 (2008) 1755-1764.

[24] T. Hong, Y. Jiang, A new multizone model for the simulation of building thermal performance, Build. Environ. 32 (1997) 123-128.

[25] Y. Zhang, X. Xie, T. Luo, et al., Building environment design simulation software DeST (4): solar radiation related models in building thermal process, Heat. Ventil. Air Condit. 34 (2004) 55-64 (in Chinese).

[26] Y. Gao, L. Zhao, J. Roux, Order reduced model of building thermal bridge dynamic additional heat loss, Heat. Ventil. Air Condit. 34 (2004), 15-19 (in Chinese).

[27] M. Wetter, Simulation model finned water-air-coil without condensation, Berkeley， CA (US): Emest Orlando Lawrence Berkeley National Laboratory，

1999.

[28] Y. Hong, Y. Sun, W. Wang, J. Liu, X. Wu, Development and validation of fan coil unit air-conditioning dynamic control process simulation platform based on Modelica, Building Science 32 (2016) 121-127 (in Chinese).

[29] GB 50189, Design standard for energy efficiency of public buildings, 2015 (in Chinese).

[30] X. Xie, F. Song, X. Zhang, et al., Building environment design simulation software DeST (11): treatment of dynamic heat transfer through underground zone, Heat. Ventil. Air Condit. 35 (2005) 55-63 (in Chinese).

[31] Y. Jiang, Generation of typical meteorological year for different climates of China, Energy 35 (2010) 1946-1953.

[32] X. Zhang, W. Chen, W. Yu, et al., Experimental study on the proportion between the convection heat and radiation heat for commonly used radiators, Heat. Ventil. Air Condit. 6 (1994) 13-15 (in Chinese).

[33] B. Xu, A. Huang, L. Fu, H. Di, Simulation and analysis on control effectiveness of TRVs in district heating systems. Energy Build. 43 (2011) 1169 -1174.

[34] ASHRAE Guideline 14, Measurement of Energy, Demand and Water Savings, 2014.

[35] Qingdao Passive House Engineering and Technology Co., LTD., Refined operation for passive house technology center in Sino-German Ecological Park, Proceedings of Tsinghua University Building Energy Conservation Forum, 2018,

Beijing (in Chinese).

[36] B. Xu, Z. Chen, X. Wang, P. Jiang, Field tests to examine energy saving effects of occupants' thermostatic radiator valves (TRVs) regulating behavior in district heating systems, Sci. Technol. Built Environ. (2022) 1-10.

[37] DB11/891, Design standard for energy efficiency of residential buildings, 2012 (in Chinese).